

## Effect of elastomeric nanoparticles on properties of phenolic resin

Hengyi Ma<sup>a,b</sup>, Genshuan Wei<sup>a</sup>, Yiqun Liu<sup>b</sup>, Xiaohong Zhang<sup>b</sup>, Jianming Gao<sup>b</sup>, Fan Huang<sup>b</sup>,  
Banghui Tan<sup>b</sup>, Zhihai Song<sup>b</sup>, Jinliang Qiao<sup>a,b,\*</sup>

<sup>a</sup>Department of Applied Chemistry, College of Chemistry and Molecular Engineering, Peking University, Beijing 100871, China

<sup>b</sup>SINOPEC Beijing Research Institute of Chemical Industry, Beijing 100013, China

Received 10 September 2004; received in revised form 15 July 2005; accepted 29 July 2005

Available online 15 August 2005

### Abstract

A new type of phenolic resin nano-composite, with excellent impact strength, flexural strength and heat resistance, is introduced in this paper. The phenolic resin is modified with organic elastomeric nanoparticles including nitrile butadiene and carboxylic nitrile butadiene rubbers. TEM images show that the elastomeric nanoparticles are uniformly dispersed in phenolic matrix with a diameter of about 100 nm. SEM photographs show that large quantity of microcracks, initiated by nanoparticles, exist on fracture surface. These microcracks can dissipate impact energy and improve the impact property of phenolic composite. FTIR analysis and curing reaction kinetics analysis confirm that the excellent thermal property is due to the existence of special interface between nanoparticles and phenolic matrix.

© 2005 Elsevier Ltd. All rights reserved.

**Keywords:** Elastomeric nanoparticles; Phenolic resin; Toughness

### 1. Introduction

Phenolic resins (PR) have been widely used as coatings, adhesives, composites, etc. due to their excellent flame resistance, heat resistance, insulativity, dimensional stability and chemical resistance. However, their application has significantly been limited by inherent brittleness. Materials used as toughening agents of PR include elastomers such as natural rubber and nitrile butadiene rubber (NBR) [1], reactive liquid polymers such as liquid nitrile butadiene [2] and carboxyl terminated butadiene acrylonitrile (CTBN) [3], plastics [4,5] such as polysulfone and polyamide, oils such as cashew nut shell liquid [6], tung oil [7] and linseed oil [8], and fibers such as glass fibers and aramid fibers [9]. The most widely used toughening agents are elastomers due to their high efficiency and low cost. However, the phenolic network is subject to deterioration in heat resistance, strengths and modulus after incorporation with elastomers and flexible compounds. Stiff aromatic heterocyclic

structures are usually introduced into PR molecules to improve its heat resistance. However, the same stiff structures will also decrease the PR toughness. Obviously, the method for toughening and heat resistance improving is incompatible.

Recently, studies on PR modification by addition of nanoparticles, including carbon nanotubes [10] and layered silicate [11,12], were reported. These nanoparticles are able to greatly improve heat resistance and stiffness of phenolic materials, but can only slightly enhance toughness. Report on modification of PR with organic nanoparticles has not been found yet. Introduced in this paper is a new kind of PR/organic nanoparticle composite, including PR/nitrile butadiene elastomeric nanoparticle (NBENP) composite and PR/carboxylic nitrile butadiene elastomeric nanoparticle (CNBENP) composite. The elastomeric nanoparticles (ENP) studied in this paper are special ultra-fine full-vulcanized powdered rubbers, prepared by a special irradiation technique [13,14]. The research results show that the impact strength of ENP toughened phenolic composite is increased greatly, and its flexural strength and heat resistance are also improved simultaneously. The ENP are uniformly dispersed in phenolic matrix with a diameter of about 100 nm. The size of dispersion phase is much smaller than that of conventional rubbers [15]. Thanks to their high toughening effect, low addition amount (less

\* Corresponding author. Address: SINOPEC Beijing Research Institute of Chemical Industry, Beijing 100013, China. Tel.: +86 10 64208677; fax: +86 10 64228661.

E-mail address: [jqiao@brici.ac.cn](mailto:jqiao@brici.ac.cn) (J. Qiao).

Table 1  
Composite formulation

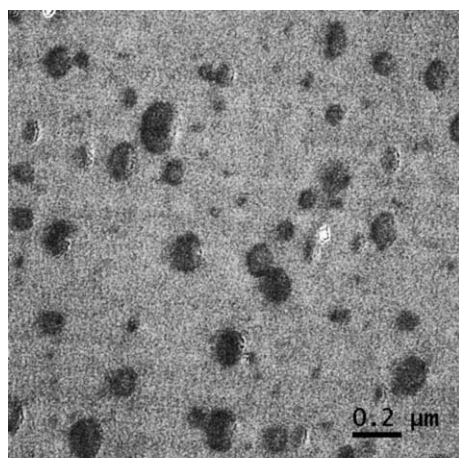
| Materials              | Percentage (wt%) |
|------------------------|------------------|
| Phenolic resin         | 43.2             |
| Wood flour             | 43.2             |
| Hexamethylenetetramine | 5.1              |
| Magnesium oxide        | 1.3              |
| Stearic acid           | 0.9              |
| Calcium carbonate      | 1.3              |
| Rubber                 | 5.0              |

than 5 wt%) and simple addition process, ENP have already found application in PR industry [16]. Details of the research results will be discussed in this paper.

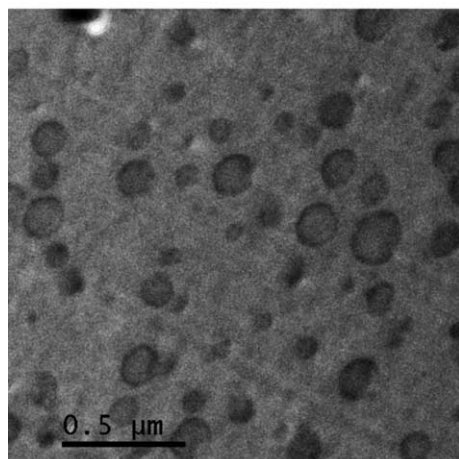
## 2. Experimental part

### 2.1. Materials

Materials used in the study are Novolac PR (SP26II) synthesized from phenol and formaldehyde by Shanghai



(a)



(b)

Fig. 1. TEM photographs of (a) PR + 5 wt% NBENP and (b) PR + 5 wt% CNBENP blends.

Shuangshu Resin Factory, China, hexamethylenetetramine (HMTA), a curing agent supplied by Beijing Yili Fine Chemical Company, China, NBENP (VP-401) and CNBENP (VP-501) with diameter about 100 nm produced by SINOPEC Beijing Research Institute of Chemical Industry, China, and wood flour with particle size smaller than 40 μm provided by Beijing Guanghua Lumber Mill, China.

### 2.2. Preparation of blends and phenolic moulding composites

The phenolic blends were prepared by blending of ENP and PR at 100–110 °C on a three-roll mill. After porphyrization, the blends were mixed with 10 phr of hexamethylenetetramine in a high-speed mixer.

The phenolic moulding composites were prepared with hot-compression molding method. The compounding formulation of phenolic moulding composite is listed in Table 1. All raw materials were thoroughly premixed in a high-speed mixer. The mixture was then blended at 100–110 °C on a three-roll mill. After porphyrization and preheating, the mixture was molded for 8 min at 170 °C under a pressure of 8 MPa. The molded samples were cut in accordance with ISO standard for mechanical tests.

### 2.3. Morphology observation of blends

Dispersion morphology of ENP in phenolic network was observed with a PHILIPS TECNAI20 transmission electronic microscope (TEM). The samples were ultramicrotomed at room temperature and were stained in  $O_3$  vapor for 10 min. The morphology of fracture surface was examined with a FEI XL-30 field emission environment scanning electronic microscope (SEM). Samples were sputter coated with a thin gold layer under vacuum situation.

### 2.4. FTIR spectrometer

The possible chemical reaction between ENP and PR was examined by FTIR. The experiments were done in a Nicolet Magna-IR760 FTIR spectrometer with a microscope attachment at a resolution of 2  $cm^{-1}$ .

### 2.5. Mechanical property measurements

The unnotched Charpy impact strength of composites was measured on a X CJ-4 impact machine according to testing standard ISO179-1. Flexural strength and modulus were measured on an INSTRON 4466 Universal Materials Testing Machine according to testing standard ISO178, and heat-distortion temperature on a 148-HDR-S heat-distortion tester according to testing standard ISO75-2.

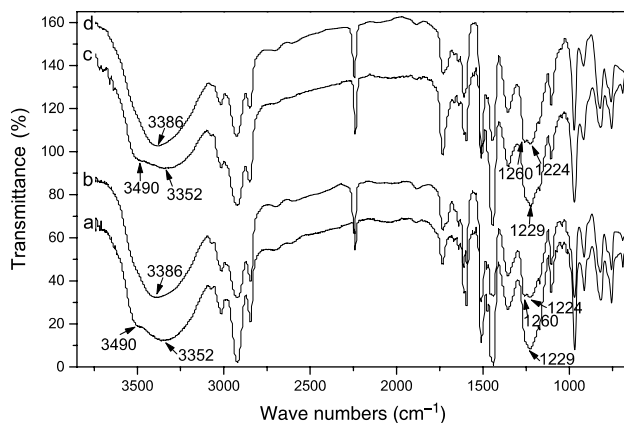


Fig. 2. FTIR spectra. (a) NBENP/PR (50/50) and (c) CNBENP/PR (50/50) before melt blending; (b) NBENP/PR (50/50) and (d) CNBENP/PR (50/50) after melt blending.

### 2.6. Thermal analysis and test of crosslinking degree

Thermal analysis was performed on a TA Q100 DSC calorimeter at constant-heating rate from 40 to 300 °C under a dry nitrogen atmosphere. The heat decomposition temperature ( $T_d$ ) was measured by thermogravimetric analysis with a Perkin–Elmer TGA-7 thermal analyzer at a heating rate of 10 °C/min from 50 to 600 °C. Crosslinking degree was measured by acetone extraction method according to GB-2576-89.

## 3. Results and discussion

### 3.1. Morphology of ENP in phenolic matrix

Fig. 1 shows the dispersion morphology of 5 wt% ENP in phenolic matrix. The rubber particles are uniformly dispersed in phenolic matrix with diameter of about 100 nm, without any aggregation. The new type of PR composite modified by ENP has a large interface because of the large specific surface area of nanoparticles. Furthermore, it is also found that the uniform dispersion of rubbers can be ensured by adequate blending time and appropriate addition amount. The aggregation of rubbers appears when ENP content is over 5 wt%; therefore, ENP addition of less than 5 wt% is recommended.

### 3.2. Reaction between PR and ENP

Fig. 2 shows the FTIR spectrums of ENP/PR mixtures before and after melt blending. The existence forms of phenolic hydroxyl group are noticeably changed after melt blending. Before melt blending, the stretching vibration of hydroxyl group shows a broad peak at 3352  $\text{cm}^{-1}$  (hydrogen bond) with a shoulder peak at 3490  $\text{cm}^{-1}$  (free hydroxyl group). After melt blending, it becomes a more symmetric peak at 3394  $\text{cm}^{-1}$ , which indicates that some hydrogen bonds are broken by ENP. Moreover, the peak at 1230  $\text{cm}^{-1}$ , which is attributed to stretching vibration of phenolic C–OH, splits and shifts to higher wavenumbers after melt blending, which implies the influence of ENP on some phenolic hydroxyl groups. It is well known that the hydrogen atoms at *ortho* or *para* position of phenolic hydroxyl group are very active. These active hydrogen atoms are subject to substitution of some active functional groups on ENP surface during melt blending. As a result of substituent reaction, crosslinked ENP, acting as a large substituent group, is introduced onto the benzene ring of PR. Therefore, the induction effect of large substituent groups causes a shift of peak at 1230  $\text{cm}^{-1}$  to higher wavenumbers. Other changes are not observed in the FTIR spectrums because only active groups on rubber surface can react with PR and the changes are too weak to appear in IR spectrum. Anyhow FTIR analysis does indicate the happening of chemical reaction between rubbers and PR during melt blending of the components and the enhancement of interfacial adhesion between ENP and PR due to chemical interaction.

### 3.3. Mechanical properties and thermal properties

Mechanical properties and thermal properties of phenolic nano-composites are shown in Table 2. It is evident in the table that impact strength, flexural strength and heat resistance are concurrently improved and CNBENP has better modifying effect than NBENP. Impact strength, flexural strength, heat distortion temperature and heat decomposition temperature of the modified composite with only 5 wt% CNBENP are increased by 67, 10%, 26 and 34 °C, respectively, compared with the unmodified composite. The reasons will be investigated in the following text.

Table 2  
Mechanical and thermal properties of phenolic moulding composites

| Composite      | Charpy impact strength (kJ/m <sup>2</sup> ) | Flexural strength (MPa) | Flexural modulus (GPa) | Heat distortion temperature (°C) | Heat decomposition temperatures (°C) |
|----------------|---|-------------------------|------------------------|----------------------------------|--------------------------------------|
| Without rubber | 5.20  | 98.5                    | 7.96                   | 141.5                            | 413.44                               |
| 5 wt% NBENP    | 7.75  | 101.0                   | 7.11                   | 160.3                            | 435.14                               |
| 5 wt% CNBENP   | 8.70  | 107.9                   | 7.36                   | 167.9                            | 446.97                               |

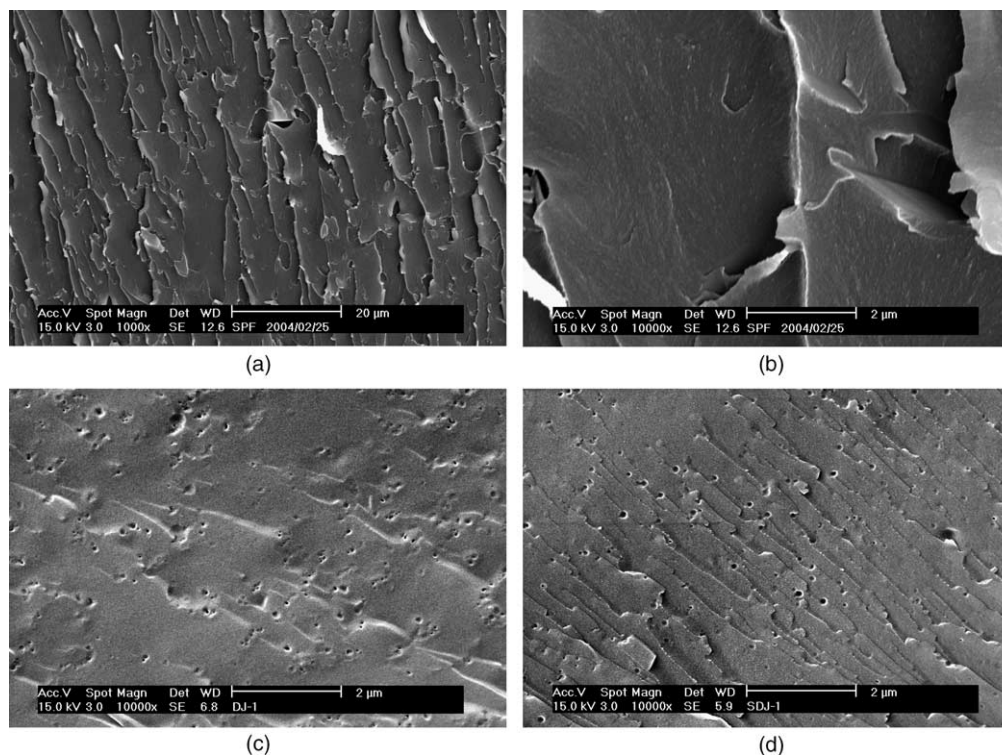


Fig. 3. SEM photographs of fracture surface of toughened phenolic network (a) and (b) un-toughened; (c) 5 wt% NBENP toughened; (d) 5 wt% CNBENP toughened.

#### 3.4. SEM observation of fracture surface of ENP modified PR

SEM photographs of impact fracture surface of ENP modified PR are shown in Fig. 3. It can be observed that the average distance between microcracks is over 5  $\mu\text{m}$  on the fracture surface of pure phenolic network, as shown in Fig. 3(a) and (b); however, the average distance between microcracks initiated by ENP is only about 0.5  $\mu\text{m}$  on the fracture surface of PR/ENP blends, as shown in Fig. 3(c) and (d). Therefore, there are much more microcracks on the fracture surface of PR/ENP blends than that on the fracture surface of pure phenolic network due to smaller distance between microcracks. It is well known that plastic deformation of the matrix is limited in thermoset plastics with high crosslink density and microcrack is a main toughening mechanism [17,18]. The amount of microcracks, initiated by rubber particles, depends on the particle size of rubber in PR/rubber composite if same amount of rubber is used; therefore, it is explanatory that the ENP toughened PR system, where rubber particle size is about 100 nm, has much more microcracks and much higher impact strength than the conventional rubber toughened PR system.

#### 3.5. Curing reaction kinetics analysis

There are two possible reasons to explain why the modified phenolic composites show excellent heat

resistance. One of them is strong adhesion on the interface between ENP and phenolic matrix because of chemical bond and large specific surface area of nanoparticles. The strong interface can inhibit deformation and decomposition of phenolic network when it is heated. Another possibility is that soft ENP can make the segmental motion of PR molecules on interface easier; which accelerates PR crosslinking and hence improves its heat resistance. To make it clear, curing reaction kinetics analysis of PR was performed by means of DSC.

Kissinger and Flynn–Wall–Ozawa methods [19,20] can be used to calculate kinetic parameters, such as the activation energy, and it is not necessary to have a prior knowledge of the reaction mechanism. In dynamic heating experiment of DSC, the maximum curing reaction rates of PR appear at different temperatures with different constant heating rate. According to the Kissinger and Flynn–Wall–Ozawa methods, the activation energy can be obtained from the temperature at maximum rate and the constant heating rate. The resulting relation of Kissinger method can be expressed as

$$\frac{d[\ln(\beta/T_p^2)]}{d[1/T_p]} = -\frac{E_1}{R} \quad (1)$$

and Flynn–Wall–Ozawa method can be expressed as

$$\lg(\beta) = \lg \left| \frac{AE_2}{g(a)R} \right| - 2.315 - \frac{0.457E_2}{RT_p} \quad (2)$$

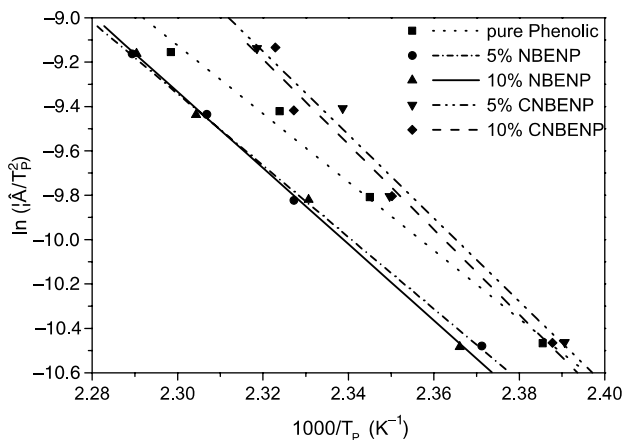


Fig. 4. Curves regressed from  $\ln(\beta/T_p^2)$  and  $1/T_p$ .

Where  $T_p$  is the temperature at maximum rate ( $^{\circ}\text{C}$ ),  $\beta = dT/dt$  is a constant heating rate ( $^{\circ}\text{C}/\text{min}$ ),  $E_1$  and  $E_2$  are the activation energies ( $\text{J}/\text{mol}$ ),  $R$  is the perfect gas constant  $8.314 \text{ J}/(\text{mol K})$ ,  $A$  is the pre-exponential factor,  $g(a)$  is the function of the curing degree  $a$ .

Dynamic heating experiments on PR, containing ENP and 10 phr of HMTA, were performed at constant heating rate of 5, 10, 15, 20  $^{\circ}\text{C}/\text{min}$ , respectively. According to the Kissinger method, a series of  $\ln(\beta/T_p^2)$  versus  $1/T_p$  gave curves (Fig. 4) by linear regression. The activation energies  $E_1$  were calculated from slope of these straight lines. Similarly, a series of  $\lg(\beta)$  versus  $1/T_p$  regressed to curves (Fig. 5) by Flynn–Wall–Ozawa method to calculate the activation energy  $E_2$ . Regression coefficients of all lines were greater than 0.995. The activation energies calculated by two methods are listed in Table 3. It is evident that the slopes of ENP modified PR increase with the increase of ENP content, as shown in Figs. 4 and 5, and their activation energies of curing reaction also increase, as shown in Table 3. The increase of activation energies caused by addition of CNBENP is more than that by NBENP. It indicates that ENP plays an inhibition role in curing reaction of PR. This result is also confirmed by measurement of

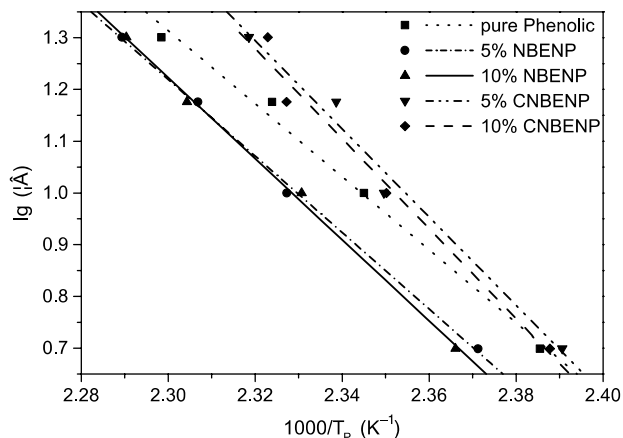


Fig. 5. Curves regressed from  $\lg(\beta)$  to  $1/T_p$ .

Table 3

Activation energies obtained by Kissinger and Flynn–Wall–Ozawa methods

| PR             | $E_1$ (kJ/mol) | $E_2$ (kJ/mol) | $\bar{E}$ (kJ/mol) |
|----------------|----------------|----------------|--------------------|
| Without rubber | 128.1          | 128.4          | 128.3              |
| 5% NBENP       | 134.4          | 134.5          | 134.5              |
| 10% NBENP      | 142.8          | 142.5          | 142.7              |
| 5% CNBENP      | 156.1          | 155.1          | 155.6              |
| 10% CNBENP     | 159.5          | 158.3          | 158.9              |

crosslinking degree, which shows that the crosslinking degree of phenolic network modified by ENP decreases when compared with pure PR (Table 4). Therefore, more possibly, the existence of special interface is the main reason for improvement of heat resistance.

#### 4. Conclusion

A new type of PR/ENP nano-composite is introduced. TEM images show that the rubber particles are uniformly dispersed in phenolic matrix with a diameter of about 100 nm. PR nano-composites, modified with 5 wt% of ENP, show simultaneous improvement on impact strength, flexural strength and heat resistance, compared with unmodified one. CNBENP shows better modifying effect than NBENP. SEM shows that large quantity of microcracks, initiated by nanoparticles, exist on fracture surface, because of the minor distance between rubber particles. More microcracks can dissipate more impact energy; therefore, having more microcracks is a main reason for the improvement of impact property in the new PR composites. The increase in activation energies of curing reaction of PR and the decrease in crosslinking degree indicate that ENP plays an inhibition role in curing reaction of PR. FTIR analysis confirms that the chemical reaction between ENP and PR takes place when they are melt blended. Therefore, the existence of special interface should be the main reason for improvement of heat resistance in the new PR composites.

#### Acknowledgement

This project was subsidized by the Special Funds for Major State Basic Research Project of China (G1999064800).

Table 4

Degree of crosslinking was measured by acetone extraction method

| Phenolic network | Degree of crosslinking (%) |
|------------------|----------------------------|
| Without rubber   | 88.1                       |
| 5 wt% NBENP      | 84.8                       |
| 5 wt% CNBENP     | 74.0                       |

**References**

- [1] Sasidharan PA, Ramaswamy R. *J Appl Polym Sci* 1998;69:1187–201.
- [2] Camino G, Alba E, Buonficio P, Vikoulov KJ. *Appl Polym Sci* 2001;82(6):1346–51.
- [3] Gouri C, Nair CP, Ramaswamy R. *J Appl Polym Sci* 1999;74(9):2321–32.
- [4] Carter JT. *Plast Rubber Compos Process Appl* 1991;16(3):157–70.
- [5] Dong R, Yang W, Qi S. *Modern Plast Process Appl* 2001;13(5):16–8.
- [6] Sathiyalekshmi K. *Bull Mater Sci* 1993;16(2):137–50.
- [7] Yu G. *Polym Mater Sci Eng* 1995;11(2):121–6.
- [8] Chakrawarti PB, Mehta V. *Indian J Technol* 1987;25(3):109–13.
- [9] Qi S, Zeng Z, Li Y. *China Plast Ind* 1999;27(6):15–16.
- [10] Su Z, Liu Y, Wei Q. *Carbon Tech* 2002;(1):8–11.
- [11] Choi MH, Chung IJ, Lee JD. *Chem Mater* 2000;12:2977–83.
- [12] Byun HY, Choi MH, Chung IJ. *Chem Mater* 2001;13:4221–6.
- [13] Liu Y, Zhang X, Wei G, Gao J, Huang F, Zhang M, et al. *Chin J Polym Sci* 2002;20(2):93–8.
- [14] Huang F, Liu Y, Zhang X, Wei G. *Macromol Rapid Commun* 2002;23:786–90.
- [15] Dutta A, Mauman EB. *Polym Mater Sci Eng* 1992;67:482–3.
- [16] Fan Z, Tan Y, Ma H, Xia Y, Ren C, Zhu D. *New Chem Mater* 2004;32(2):35–7.
- [17] Lu F, Plummer CJG, Cantwell WJ, Kausch HH. *Polym Bull* 1996;37:399–406.
- [18] Shiann HL, Nauman EB. *J Mater Sci* 1991;26:6581–90.
- [19] Xu W, Bao S, Shen S, Tang S, He P. *Acta Polym Sinica* 2002;(4):457–61.
- [20] Lopez J, Lopez-Bueno I, Nogueita P. *Polymer* 2001;42:1669–77.